DYNAMICS OF CONFINED MOLECULAR SYSTEMS

By modeling restricted geometries with well-characterized porous silica glasses, experimenters can determine a single geometric parameter that relates finite-size effects to observed dynamic and thermodynamic behavior.

J. M. Drake and J. Klafter

The dynamic and thermodynamic properties of molecular systems are known to be modified by confinement in very small spaces. However, making explicit and unambiguous connections between the geometry of the confining space and the molecular behavior has proven to be difficult, and the connections, when made, are frequently controversial. Nonetheless studies show that within a family of similarly prepared porous materials, the effect of finite size on the behavior of confined liquids and gases scales with a single geometric property of the pore space.

Systems characterized by spatial restrictions and low dimensions-such as zeolites, membranes, polymers, and porous glasses and minerals-are often found in applications where the pore diffusion of gases is a key underlying process (as in some types of heterogeneous catalysis), or where liquid diffusion through porous media is important (as in various chemical separation processes). The key issues, then, in understanding these processes—which are fundamental to new developments in such diverse fields as medicine, biochemical engineering and petroleum engineering, to mention only a few-are several: What properties of the porous medium, such as size, surface area or the chemical nature of the interface, permit selective separation? What properties of the medium affect molecular transport? What effect does finite size have on the basic properties of liquids and gases (for example, viscosity or freezing point), and at what point does hydrodynamic behavior break down?

In this article we focus attention on models of restricted geometries that have proven to be ideally suited to the study of confined liquids and gases—namely porous

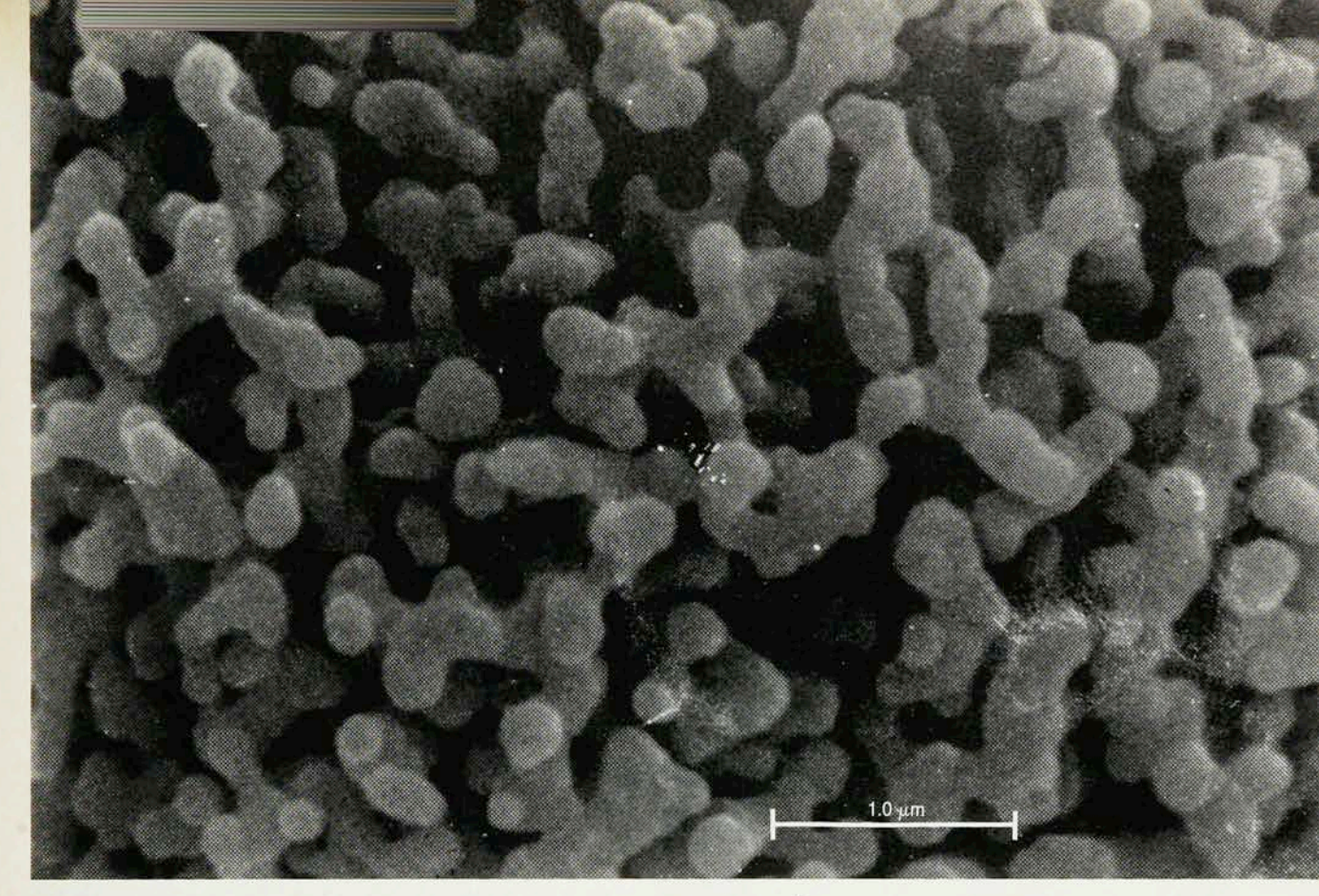
J. M. Drake is a scientist at Exxon Research and Engineering Company, Annandale, New Jersey. **J. Klafter** is a professor at the School of Chemistry at Tel Aviv University.

silica glasses, which make up a large class of materials used throughout the chemical industry. We present examples of studies that attempt to connect the dynamic and thermodynamic features of confined molecular systems to a single geometric characteristic of the confining medium: its mean pore size. Because the pores of these glasses have large internal surface areas, we pay special attention to the microscopic structure of the pore surface and give examples that show how modifying the chemical nature of the interface can change its adsorption and wetting properties. Although researchers have examined these systems by a variety of techniques, we highlight studies based on the use of several types of short-pulselaser optical probes. As we shall see, different optical techniques can give pictures of different length scales within the porous glass and can therefore provide a direct measure of the degree to which the properties of confined liquids and gases scale with the mean pore size.

Model systems

Researchers in many disciplines use porous silica glasses as model restricted geometries to study the dynamic and thermodynamic properties of confined molecular systems. Because these glasses are optically transparent, they are ideally suited for probe measurements with short-pulse lasers. In addition, these glasses are mechanically stable and chemically inert to many commonly used solvents.

By varying the method of preparation, one can create glasses that have a broad range of morphological features. The intraparticle pore space of these glasses is characterized by a pore size distribution that peaks around a mean pore radius $R_{\rm p}$, which can be as small as 20 Å or as large as 2000 Å. The interfacial pore surface area S also varies over three decades, approaching 1000 square meters per gram for microporous glasses and 1 m²/g for macroporous areas. $R_{\rm p}$ and S/V, the ratio of the pore surface area to



Porous silica glass Si-4000, with a mean pore radius R_p of 2000 Å, as seen by scanning electron microscopy. **Figure 1**

the pore volume, are the most important parameters characterizing the geometric features of a porous glass.

Of the many commercially available porous glasses, one has received considerable attention over the last 40 years: the phase-separated borosilicate glass made by Corning and known by the tradename Vycor. This glass is prepared from a melt with a typical composition of 75% ${\rm SiO_2}$, 20% ${\rm B_2O_3}$ and 5% ${\rm Na_2O}$. When quenched near the consolute (or critical) temperature (inside the immiscibility gap, where the phases begin to separate), this melt can form silica-rich and boron-rich phases. Removing the boron phase by acid leaching leaves a well-defined, highly connected pore network with a pseudoperiodic structure. Figure 1, an electron micrograph of a sample of silica Si-4000 ($R_{\rm p} \simeq 2000$ Å), reveals a random homogeneous pore network that looks as if it were created by the sintering of spherical glass particles.

Porous silica can also be prepared by sol-gel techniques. Starting from a sol or solution, one uses an aggregation or polymerization growth process to form a gel. The gel state can be processed further thermally to extend the range of geometric properties of the final glass. Merle W. Shafer, David D. Awschalom and James Warnock prepare sol-gel glasses by the hydrolysis of alkoxides and the gelling of colloidal silicas.² This approach leads to a series of well-characterized porous glasses with a broad range of pore sizes and surface-areato-volume ratios. Commercially prepared sol-gel glasses, are available with a variety of pore sizes and S/V values, and can also be used to study the behavior of molecular systems in restricted geometries.

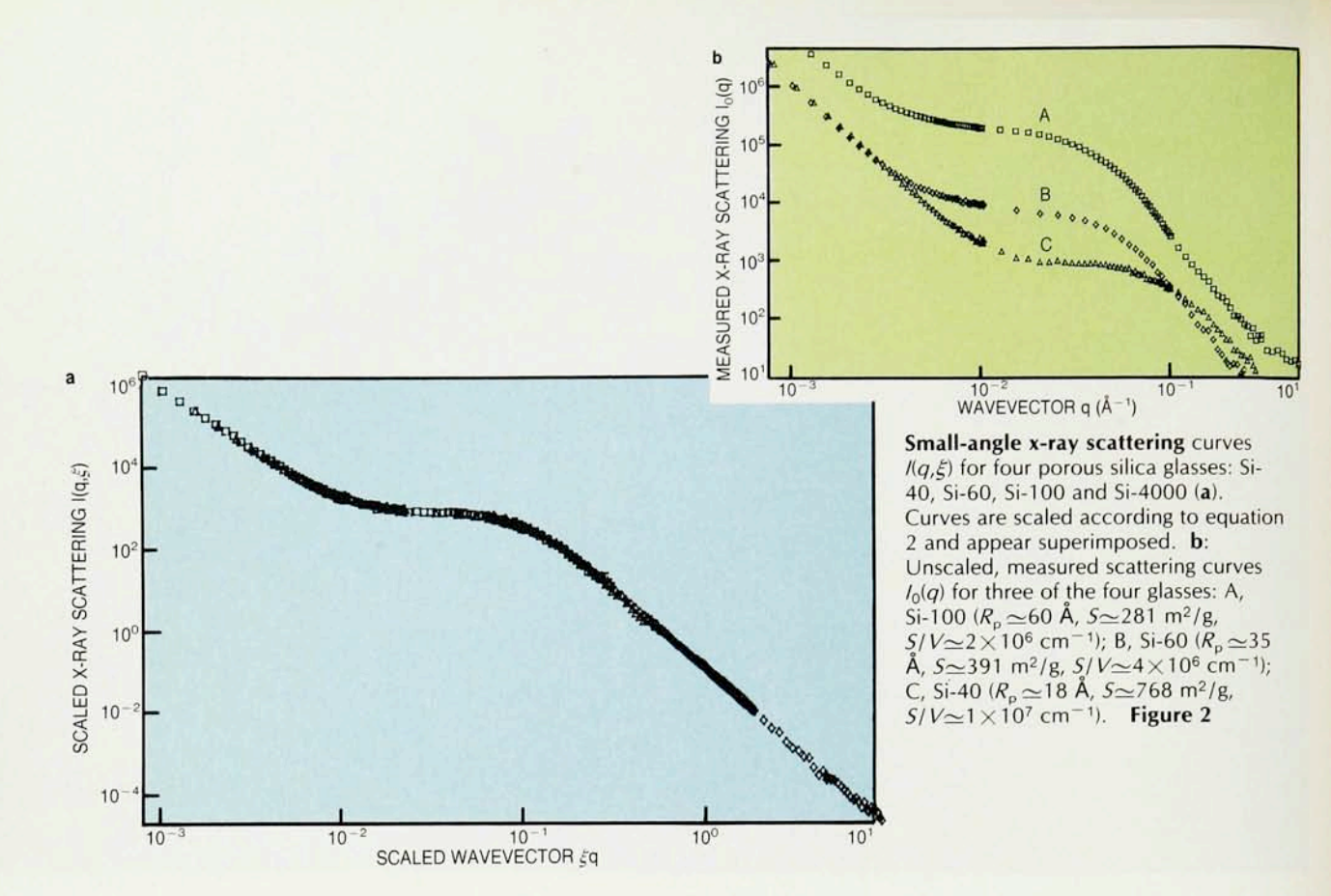
A difficult problem in using these materials to study

dynamic and thermodynamic processes of confined molecular systems is the separation of the role of finite-size effects associated with $R_{\rm p}$ from the influence of the pore surface. In confined systems the surface often introduces spatial inhomogeneity in the concentration of solute and solvent molecules due to specific molecular interactions at the pore boundary, such as wetting, adsorption or chemical reaction. Frequently the characterization of porous glasses is neglected or is problematic, complicating the interpretation of experimental results from such systems. Problems associated with surface effects are far less significant when conducting similar studies in homogeneous environments.

Therefore the use of porous silica glasses as model restricted geometries requires investigators to invest considerable time and effort in characterizing both the mesoscopic and microscopic structures of the glasses. Experimenters have used a variety of techniques to make such characterizations³:

 \triangleright Measuring the adsorption properties of gases and liquids—particularly the adsorption and desorption of N_2 at 77 K—has a long history as a method for determining the accessible pore surface area, pore size distribution and saturated pore volume. Although not always reliable for very small or large pores, adsorption studies can provide a useful starting point in characterizing porous silica glasses.

 \triangleright Mercury porosimetry can also be used to measure pore size, volume distribution and volume porosity ϕ_v ; specific surface area; and particle size distribution. Because this technique relies on the intrusion of mercury under pressure, difficulties can arise from incomplete intrusion



or from compressibility of the solid.

▷ Electron microscopy, both scanning and transmission, can be used to visualize the detailed structure of the mass and its boundary in silica glasses. When sufficient resolution is available and the structure of the material remains intact after the sample is mounted, the resulting digitized image can provide much of the same information as the two preceding techniques.

Description Small-angle x-ray and neutron scattering have also provided structural information on porous glasses.⁴ Using SAXS one can conveniently study the structure of these materials on many length scales.

A drawback of each of these techniques is that to interpret the data, one requires either a model or some additional corroborating information. However, applying all of these techniques together can provide useful and sometimes detailed structural pictures of porous silica glasses.

Correlating geometry and scattering

As part of an effort to further characterize the space-filling morphology of a family of porous silica glasses, recent SAXS studies have been used to identify a characteristic length in the glasses, $\xi=R_{\rm p}$, which appears to scale their general morphological features over a range of structural parameters—mean pore radii between 18 and 2000 Å and pore surface areas from 770 to $20~{\rm m^2/g}$. In other words, within a series of similarly prepared porous silica glasses, although the characteristic radius varies, the overall geometric properties are essentially identical.

For a three-dimensional, isotropic, random, porous medium, we can use autocorrelation functions to obtain the probability of encountering a void (the mass autocorrelation function) or an interface (the surface autocorrelation function) at certain distances from a given point, the "origin." The mass autocorrelation function $\Gamma_{_{V}}(\mathbf{r})$ is defined as

$$\Gamma_{\rm v}(\mathbf{r}) = \frac{1}{4\pi V} \int_{4\pi} \! \left[\psi_{\rm m}(\mathbf{r})^* \; \psi_{\rm m}(\mathbf{r}) \right] \! \mathrm{d}\Omega$$

where $\psi_m(\mathbf{r})$ equals 1 in the solid and 0 everywhere else. The surface autocorrelation function can be defined similarly:

$$\Gamma_{\rm s}(\mathbf{r}) = \frac{1}{4\pi V} \int_{\Lambda_{\rm s}} [\psi_{\rm s}(\mathbf{r})^* \psi_{\rm s}(\mathbf{r})] d\Omega$$

where $\psi_s(\mathbf{r})$ equals 1 along the surface of the mass and 0 elsewhere. Below we demonstrate that the mass autocorrelation function can be used to calculate the SAXS spectrum. (Later we show that the surface autocorrelation function is related to the properties of direct energy transfer in these materials.)

The observed SAXS pattern can be related to the structure of the glass through the density fluctuation autocorrelation function, which differs from the mass autocorrelation function by a constant:

$$\langle \mu_{\mathbf{v}}(\mathbf{0}) \cdot \mu_{\mathbf{v}}(\mathbf{r}) \rangle = \Gamma_{\mathbf{v}}(\mathbf{r}) - (1 - \phi_{\mathbf{v}}^{2})$$

where $\mu_{\rm v}({\bf r})$ is the density term; $\mu_{\rm v}({\bf r})$ equals 1 in the solid and 0 in the void. The SAXS spectrum I(q)—where q, a function of the scattering angle, is proportional to the inverse wavelength—can then be calculated using

$$I(q) \propto \frac{-1}{q} \frac{\mathrm{d}}{\mathrm{d}q} \mathrm{Re} \left[\int_0^\infty \mathrm{d}\mathbf{r} \langle \mu_{\mathbf{v}}(\mathbf{0}) \cdot \mu_{\mathbf{v}}(\mathbf{r}) \rangle \exp(\mathrm{i}qr) \right] \tag{1}$$

Pierre Levitz and coworkers have recently demonstrated the validity of this approach by calculating the x-ray spectrum using equation 1 and the binary data from a digitized, high-resolution transmission electron microPore interface of a silica glass that has been chemically modified by a linear alcohol. Red circles represent the —CH₂—O— functional groups, and green lines represent the alkyl chains, which extend into the pore region (deep blue). Figure 3

graph image of an ultrathin section of a porous glass.⁴ The calculated spectrum compares favorably with the measured spectrum.

Another, more common way to correlate SAXS and the characteristic scale length of the glasses is to inspect the behavior of I(q) and analyze one of the asymptotic limits as power-law scattering,

$$I(q) \propto q^{-\beta}$$

As shown by G. Porod in 1951 for porous materials, in which the scattering is dominated by the surface of the pore, for smooth surfaces $\beta=4$ at large q. Silica glasses exhibit⁵ a $\beta=4$ power-law scattering for values of $q\xi$ greater than 1, the scattering regime in which SAXS is sensitive to length scales on the order of the mean distance between interfaces. Thus in the $\beta=4$ power-law scattering regime SAXS probes the morphology of a single pore. On the other hand, for $q\xi$ less than 1 SAXS is sensitive to the organization of many pores—the structure of the mass itself.

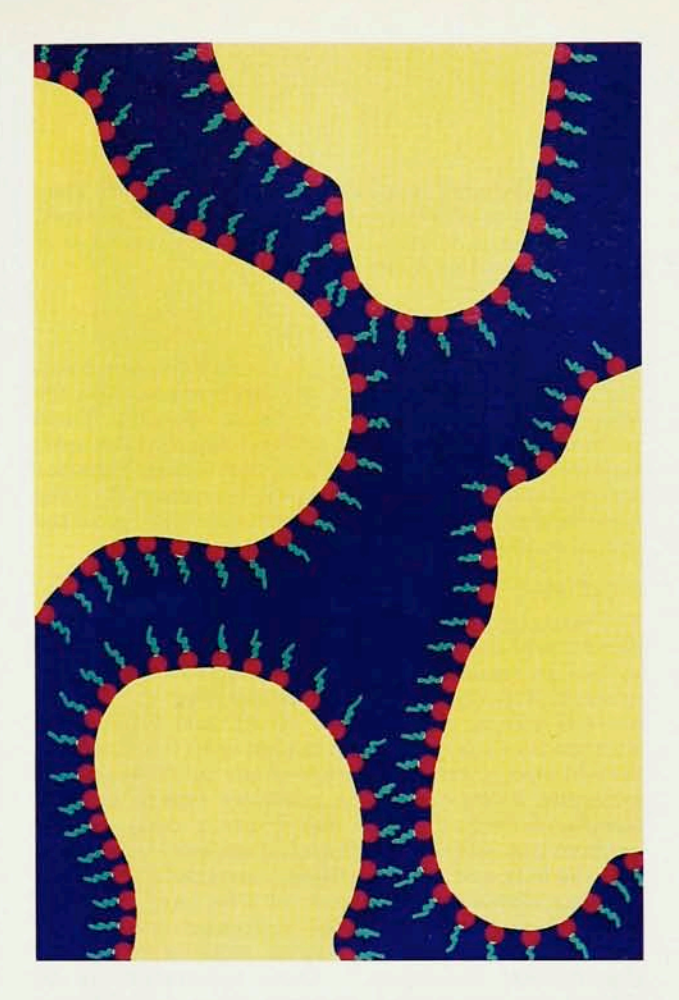
The exponent β need not, however, be an integer. S. K. Sinha and Robin Ball⁶ have generalized the meaning of the power-law exponent for scattering from porous materials by relating β to the fractal dimension d_m of the spatial organization of the mass while concurrently treating the surface of the mass as a fractal of dimension d_n :

$$\beta = d_s - 2d_m$$

According to this interpretation, a fractally rough interface is responsible for non-Porod ($\beta \neq 4$) exponents.

Scattering scales with pore size

The scaled x-ray scattering from four porous silica glasses in a homologous series is shown in figure 2. The scattering pattern reveals three characteristic regions in q. At large q, where $q\xi$ is greater than 1, there is a "Porod-like" powerlaw scattering, characterized by an exponent of 4. This Porod-like behavior is a general characteristic of these silicas and indicates that the surface of the pore scatters like a random smooth interface and not like a fractal surface. In fact, $\beta = 4$ is consistent with Sinha and Ball's generalization of the power-law exponent, because for a smooth Euclidean surface $d_{\rm s}=2$, and for a homogeneous distribution of mass $d_{\rm m}=3$. (There are samples where the exponent departs from 4, as shown in the inset of figure 2, but the length scale for this departure, $q\xi \geqslant 10$, approaches the atomic scale. Because the scattering intensity is weakest on the atomic scale, it is difficult to interpret the scattering for this region.) At small q, above the plateau $q\xi < 1$, a second power region appears. This scattering is from structures in the glass that are larger than R_p . The exponent for this power-law scattering is often approximately 3, but the origin of this scattering is not well understood.



The plateau seen in I(q), which occurs for q near $2R_{\rm p}$, is a common feature of all these porous glasses. It has been shown by Drake, Levitz and Sinha that the overall scattering features for a group of silicas having mean pore sizes ranging from roughly 20 to 2000 Å scales with their characteristic pore size as

$$I(q,\xi) = I_0(\xi) F(q\xi) \tag{2}$$

where the value of ξ is obtained from N_2 desorption measurements.7 The SAXS curves for four different glasses, shown superimposed in figure 2, were scaled according to equation 2. This scaling relationship has been shown to hold for other porous silica glasses by Paul W. Schmidt and coworkers.8 That such a scaling relationship holds even approximately over such a large range in $R_{\rm p}$ suggests that the morphological features of these materials must remain unchanged as R_p and S vary over two decades. We may therefore infer that the electron micrograph of Si-4000 (figure 1) characterizes the spacefilling organization in the entire series of porous glasses: an isotropic, random space-filling mass whose structure suggests a growth process based on the aggregation of spherical particles and having, as also suggested by the SAXS data, a smooth pore interface.

Because a single length $R_{\rm p}$ scales the general morphology for a family of porous glasses, these materials are ideally suited for studying the effect of the size of the spaces confining molecular systems on their dynamic and thermodynamic properties. Warnock, Awschalom and Shafer, using sol–gel glasses to study the geometrical supercooling of liquid oxygen, demonstrated how $R_{\rm p}$ scales

the thermodynamic properties of a confined liquid. They showed that the freezing-point depression ΔT of confined liquid oxygen is determined by the characteristic size of the space according to the relationship

$$\Delta T = \frac{2\Delta\sigma \ V_{\rm m} \ T_0}{\Delta h_{\rm f} \ R_{\rm p}}$$

where $\Delta h_{\rm f}$ is the heat of fusion, T_0 the bulk freezing point, $V_{\rm m}$ the molar volume and $\Delta\sigma$ the difference between the solid-wall and liquid-wall interfacial energies. These researchers have observed that this relationship also holds for ethanol. Their results suggest that similar behavior will be found in other porous materials for which $R_{\rm p}$ is the important scale length that characterizes the size of the spatial confinement.

Modifying the pore interface

The thermodynamics of a confined liquid can be shown to depend explicitly on R_p . Are the dynamic properties of molecular liquids also affected by confinement? The dynamic properties of liquids are in fact affected by both finite-size effects, characterized by R_p , and interactions with the pore interface. In an environment that has large surface area, a high percentage of the solute or solvent molecules interact with the container interface. Such significant surface interactions create a concentration gradient that extends from the interface tens of angstroms into the bulk and often partitions the molecular population into distinct regions, each with its own dynamical features. One can study the molecular dynamics of systems in restricted geometries using a variety of experimental techniques.10 These techniques can be divided into two general categories: those that measure the behavior of the bulk liquid or gas directly, and those from which one infers the behavior of the bulk from the dynamical properties of a low concentration of probe molecules. While the underlying physical laws describing the dynamics are the same for both, the specifics of each molecular system must be well known and understood in the homogeneous limit (that is, where S/V approaches zero).

Mean pore size of Vycor derivatized with C_1 – C_{10} linear alcohols (red dots) and C_8 – C_{18} alkylsiloxanes (black dots) is roughly proportional to the number of alkane-chain carbons n. The inset illustrates how N_2 desorption studies can reveal the mean pore sizes in underivatized (nude) and C_{10} -derivatized porous glasses. The Kelvin equation relates pore volume V_p to R_p . Figure 4

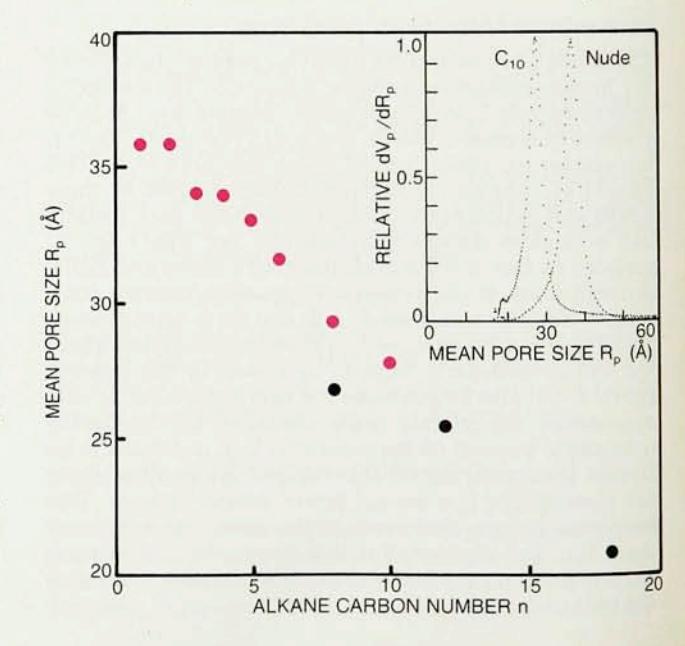
Although the properties of the pore interface are by themselves of considerable scientific interest (for example, in the study of gas adsorption, liquid adsorption, capillary condensation or wetting), the interface can sometimes be modified in a systematic way to reduce its specific chemical influence on confined liquids. In one successful method of modifying the pore interface, hydrocarbon molecules are bonded to the chemically active SiO2 surface sites. The most commonly used functionalizing reagents are alcohols and alkylsiloxanes with alkane tails. Through the use of functionalized hydrocarbon chains of varying lengths, the new derivatized surface can be made to extend between 3 and 25 Å into the pore space. The derivatized pore surface, which is now hydrophobic rather than hydrophilic, is represented schematically in figure 3. Recent work by Drake and Jack Johnson, at Exxon Research and Engineering, shows that derivatizing the pore interface with molecules of varying chain lengths not only modifies the chemical nature of the interface but also makes it possible to vary R_p systematically for any single porous glass, thus increasing the usefulness of these materials as model restricted geometries. Figure 4 shows how the mean pore size diminishes uniformly with increasing hydrocarbon chain length for Vycor derivatized with C₁-C₁₀ linear alcohols or C₈-C₁₈ alkylsiloxanes.

Viscosity of confined liquids

The question of whether the viscosity of a liquid in a pore is different than that of the bulk liquid is particularly important when one is attempting to describe molecular transport and reactions in porous materials. The simplest and most direct way to relate the diffusion coefficient D and the viscosity η in transport problems in liquids is through the Stokes–Einstein relation

$$D = \frac{k_{\rm B}\,T}{\eta 6\pi r_{\rm m}}$$

which describes the hydrodynamic behavior, as a function of temperature, of spherical objects of radius $r_{\rm m}$ in a liquid of viscosity η . One approach to measuring the viscosity of a confined liquid is to relate the rotational time $\tau_{\rm r}$ of the



Fluorescence depolarization (a) of 1×10^{-6} molar rhodamine 6G in acetonitrile in Vycor that has been modified with 1-hexanol (n=6). The spike near the origin represents the instrument response to the excitation pulse. In **b**, the rotation correlation time τ_r of rhodamine 6G dissolved in acetonitrile in Vycor is normalized to the bulk value and plotted as a function of mean pore size for C_1 – C_{10} -derivatized pores. The shaded region indicates the range of pore sizes for which rotation is strongly hindered. The inset depicts adsorption isotherms of rhodamine 6G in acetonitrile in derivatized and nude vycor glasses. **Figure 5**

solvent or solute molecule to η through the Stokes–Einstein–Debye equation

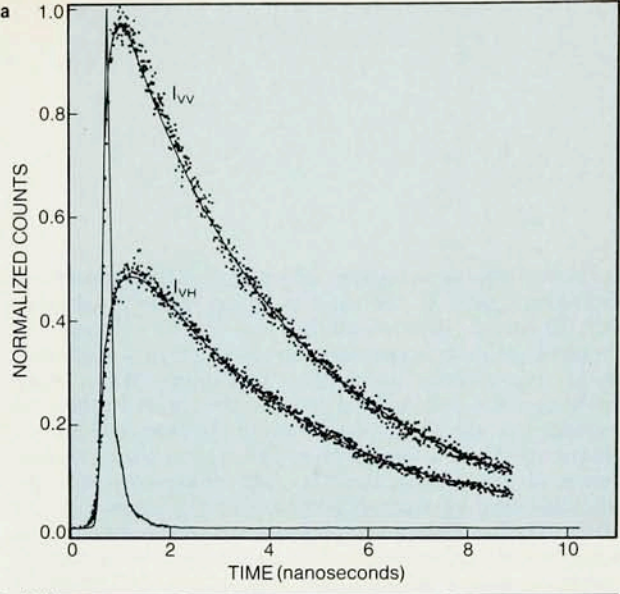
$$\tau_{\rm r} = \frac{\eta v_{\rm m} f}{k_{\rm R} T} \tag{3}$$

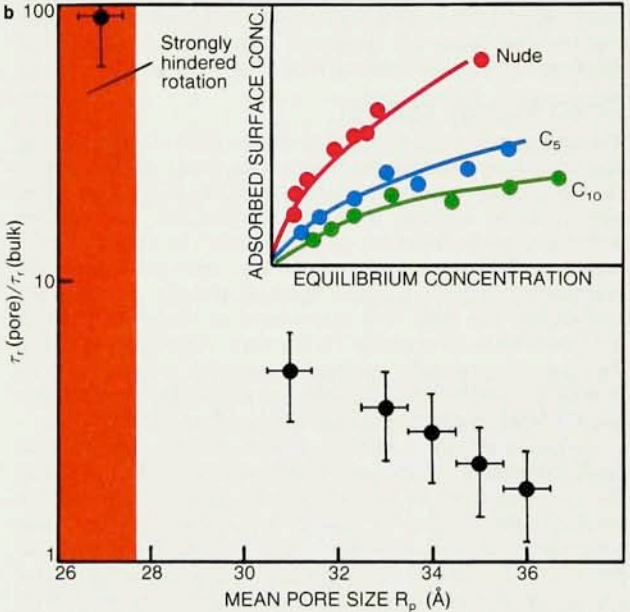
where f=1 in the case of a spherical molecule, but can be adjusted for the correct shape and boundary conditions of the diffusing molecule; $v_{\rm m}$ is the molecule's hydrodynamic volume.

Two distinct problems can be addressed through measurements of τ_r . In one approach τ_r , which should be related to the viscosity when the Stokes-Einstein-Debye approximation strictly applies, is measured directly on a neat liquid. In another approach, one measures the rotational time of a probe molecule (at very low concentration) in a continuum of solvent molecules. Again, if equation 3 applies, both approaches should provide similar information on η . The common experience is that the approximations needed to apply equation 3 often break down, and one must consider issues relating to the molecular free volume, nonstick boundary conditions and corrections for the nonspherical nature of molecules. Below we consider sets of experimental results for each of the above-mentioned approaches.

Warnock and coworkers,11 using a subpicosecond optical birefringence technique, measured τ_r for carbon disulfide (CS2) and nitrobenzene (C6H5NO2) as neat liquids in a series of porous sol-gel glasses. Their results for CS2 in a family of glasses where $2R_{\rm p}$ was varied from 44 to 375 Å clearly show that $\tau_{\rm r}$ does not change with $R_{\rm p}$ but retains its bulk value, 1.5 picoseconds. However, for nitrobenzene in underivatized glasses τ_r could not be described by a simple exponential but rather had a biexponential behavior. Setting one exponential to the value of τ_r in the bulk, Warnock and coworkers recovered a second time, τ_r^* , which describes the hindered rotation of the nitrobenzene confined to a layer near the pore interface in an underivatized glass. The interfacial nitrobenzene layer was estimated to be 12 Å thick, and the value of τ_r^* suggested that the viscosity of nitrobenzene near the wall is three times that of the bulk. When the pore interface was derivatized with ethanol, τ_r was again described by a simple exponential equal to the bulk value of 38.6 psec. Thus in these two examples there is no clear evidence of τ_r scaling with R_p . Probes with short time scales are sensitive to small length scales and, as shown here, provide little clue of the nature of the pore when they are sensitive to a length scale much smaller than R_p .

In the alternative case, where a fluorescent probe molecule is dissolved in a solvent, the authors measure the rotational time of the solute by a polarized picosecond laser-pulse technique and follow the time evolution of fluorescence depolarization. We use an optical probe with a well-known bulk τ_r —the dye molecule rhodamine 6G. Using a series of derivatized porous Vycor glasses, we can





study the local viscosity experienced by the probe as $R_{\rm p}$ is changed systematically. The solvent, acetonitrile (CH₃CN), a nonassociating (aprotic, nonhydrogen-bonding) polar solvent, is repelled by the nonpolar hydrocarbon layer, and an interface is created between the two immiscible phases: Both the probe and the solvent are expected to be excluded from the derivatized layer.

The molecular reorientation time is obtained from measurements of the vertical and horizontal components of the polarized fluorescence decay, $I_{\rm VV}(t)$ and $I_{\rm VH}(t)$ as shown in figure 5a. In the limit of simple well-behaved systems, $\tau_{\rm r}$ is related to the measured quantities $I_{\rm VV}(t)$ and $I_{\rm VH}(t)$ through the polarization anisotropy r(t):

$$\begin{split} r(t) = & \frac{I_{\mathrm{VV}}(t) - I_{\mathrm{VH}}(t)}{I_{\mathrm{VV}}(t) + 2I_{\mathrm{VH}}(t)} \\ = & r_0 \, \exp(-t/\tau_{\mathrm{r}}) \end{split} \label{eq:relation_relation}$$

where r_0 is the steady-state anisotropy. In this system a small population of probe molecules is bound to the Vycor surface at vacancies formed at random underivatized sites. The presence of adsorbed probes adds a second exponential

term to the polarization anisotropy. The adsorption isotherm, shown in the inset to figure 5b, for rhodamine 6G (dissolved in acetonitrile) on Vycor confirm the existence of surface vacancies for some derivatized glasses. While recognizing that a small percentage of the probe molecules are immobilized because they are adsorbed, we assume that the probe population in the pore is randomly distributed in the liquid; thus the results illustrated in figure 5b are quite dramatic. The data show that the effective local viscosity experienced by the probe is larger than in bulk solution and increases as the pore volume is systematically decreased. This result is at least qualitatively consistent with the idea that in the limit at which the hydrodynamic radius approaches the size of the pore radius-the "strongly hindered" regime-the simple hydrodynamic picture may no longer strictly apply.12

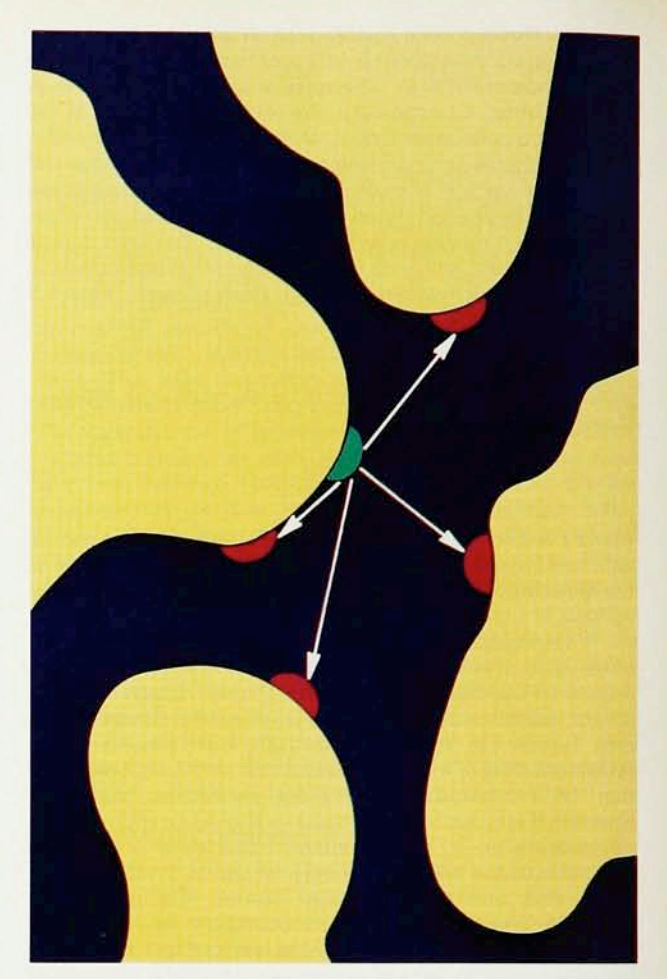
Direct energy transfer

We now connect the structural details of the model porous systems to dynamical processes that occur within them. As the mass autocorrelation function $\Gamma_{\rm v}({\bf r})$ has been shown to be related to SAXS intensities, the surface autocorrelation function can be related to direct energy transfer. Direct energy transfer is a resonant transfer of electronic excitation from excited donors to acceptor molecules; the idea was introduced as early as 1949 in studies of bulk solution by Th. Förster. Applications of the direct-energy-transfer method to complex systems such as porous glasses provide an additional tool for characterizing the spatial distribution of the pore interface.

The basic idea behind direct energy transfer in confined systems, shown schematically in figure 6, is to tag the pore surfaces of a transparent porous glass with a random distribution of donor molecules (at very low concentration) and acceptor molecules (at 100 times the donor concentration). A donor is initially excited, and the excitation is transferred to the acceptors with rates W(r) that depend on the donor–acceptor distance r. At the low concentration of donors used, excitation transfer among them is insignificant. In this type of experiment one follows the time evolution of the fluorescence of the donor. One generally chooses a donor–acceptor pair that is characterized by dipole–dipole interactions and therefore has an energy transfer rate

$$W(r) = \left(\frac{R_0}{r}\right)^6 \frac{1}{\tau_t}$$

where $\tau_{\rm f}$ is the fluorescence lifetime of the isolated donor and R_0 is the critical Förster radius, the donor–acceptor distance at which the energy transfer rate equals the fluorescence decay rate ${\tau_{\rm f}}^{-1}$. R_0 provides an estimate for the length scale over which direct energy transfer is a sensitive probe. It is this length scale that, together with $R_{\rm p}$, determines the characteristics of the donor relaxation in each of the series of porous silicas. A more realistic length scale, which takes experimental conditions into account, is $R_{\rm max}$, equal in this case to approximately $1.5R_0$. This length scale, which acts in these studies as an "optical yardstick," provides a picture of a slightly larger area than



Direct energy transfer in a pore from an excited donor molecule (green) to nearby acceptor molecules (red). **Figure 6**

does the "rotational yardstick."

The fluorescence decay pattern $\Phi(t)$ of the donor is generally given by 13

$$\Phi(t) = \exp\left[-\frac{t}{\tau_c} - p \int d\mathbf{r} \, \rho(\mathbf{r}) \{1 - \exp[-tW(r)]\}\right]$$
 (4)

where p is the density of acceptors (and is much less than 1) and $\rho(\mathbf{r})$ is the site-density function, which is related to the surface autocorrelation function. Figure 7 shows the observed fluorescence decay for Si-100. The upper curve represents the decay of an isolated donor on the surface, and the lower curve shows the decay in the presence of acceptors. Equation 4 is central to the relationship between the dynamical observable $\Phi(t)$ and the structural information folded into $\rho(\mathbf{r})$. There are two ways to interpret the relationship between the fluorescence relaxation and $\rho(\mathbf{r})$: \triangleright In the case of fractal surfaces of dimension d_s , $\rho(\mathbf{r})$ is proportional to r^{d_s-3} . The donor relaxes according to

$$\Phi(t) = \exp\left[(-t/\tau_{\rm f}) - At^{d_{\rm s}/6}\right]$$
 (5)

where A is time independent. Equation 5 connects the decay pattern $\Phi(t)$ to the surface geometry described through $d_{\rm s}$. This equation has been extensively applied by various groups in the study of porous systems and various molecular assemblies.¹⁰

 \triangleright For regularly shaped pores equation 4 yields temporal crossovers that depend on the local length scales R_p and

 R_0 . As an example consider an often-used model for simple pores: an infinite cylindrical pore of radius $R_{\rm p}$ with donor and acceptor molecules randomly distributed on its surface. From such a system one obtains a two-dimensional decay pattern at short times, corresponding to energy transfer to acceptors close to the donor. At longer times the decay crosses over to one-dimensional behavior. In terms of equation 5 this means that one should observe the Euclidean limits $d_{\rm s}=2$ and $d_{\rm s}=1$ for short and long times, respectively. The crossover itself is determined by the lengths $R_{\rm s}$ and $R_{\rm s}$:

times, respectively. The crossover itself is defined the lengths
$$R_{\rm p}$$
 and $R_{\rm 0}$:
$$\Phi(t) \sim \left\{ \begin{array}{ll} \exp[\,-\,Bt^{1/3}]\,, & t < \tau_{\rm f}(R_{\rm p}\,/R_{\rm 0})^6 \\ \exp[\,-\,Ct^{1/6}]\,, & t \gg \tau_{\rm f}(R_{\rm p}\,/R_{\rm 0})^6 \end{array} \right.$$

Such crossovers, because they depend on $R_{\rm p}$, are finger-prints of the spatial restrictions. Nonetheless the decays over certain limited time windows may be fit to equation 5 with a noninteger $d_{\rm s}$. However, a noninteger $d_{\rm s}$ does not imply that these surfaces are fractal in nature, but result from a time averaging of the Euclidean limits.

Direct-energy-transfer experiments have been carried out on the characterized family of porous silicas Si-40, Si-60 and Si-100, with rhodamine 6G and malachite green as the donor-acceptor pair. 4 Because R_0 for this pair is 57 Å, direct energy transfer senses lengths up to 85 Å (R_{max}) . Fitting the results for the three porous glasses to equation 5 produces $d_{\rm s}$ values of 2 for Si-100 and Si-60, and 3 for Si-40; these numbers represent the regular Euclidean limits of equation 5. The relationship between R_p (from structural characterization) and $R_{\rm max}$ (the optical yardstick), which determines what features of the morphology are probed by direct energy transfer, makes it possible to corroborate these results with the characterization studies for these systems. When $R_{\rm p}$ is greater than $R_{\rm p}$ only length scales less than $R_{\rm p}$ are probed by direct energy transfer. The two-dimensional energy transfer behavior suggests that the pore surface is smooth. When $R_{\scriptscriptstyle \mathrm{D}}$ is less than $R_{
m max}$ interpore direct energy transfer exhibits $d_{
m s}=3$ behavior, as shown above.

The Knudsen regime

When gas molecules are spatially confined within pores, two scattering processes have to be considered: molecule-molecule scattering, which has a mean free path $l=k_{\rm B}\,T/\sqrt{2}\pi\sigma^2P$ where σ is the collision diameter of the molecules and P is the gas pressure; and molecule-boundary scattering, dominated by the pore size $R_{\rm p}$. Here we ignore contributions of adsorbed molecules that diffuse along the surface. The regime established at pressures low enough and pore sizes small enough that the mean free path is much larger than the mean pore size is called the Knudsen regime. Under such conditions the molecules scatter more often from the boundaries than from one another. Thus in this limit the geometry, again through the scale length $R_{\rm p}$, determines the molecular diffusion 15

$$D_{\rm K} = \frac{1}{6} g \langle v \rangle R_{\rm p} \tag{6}$$

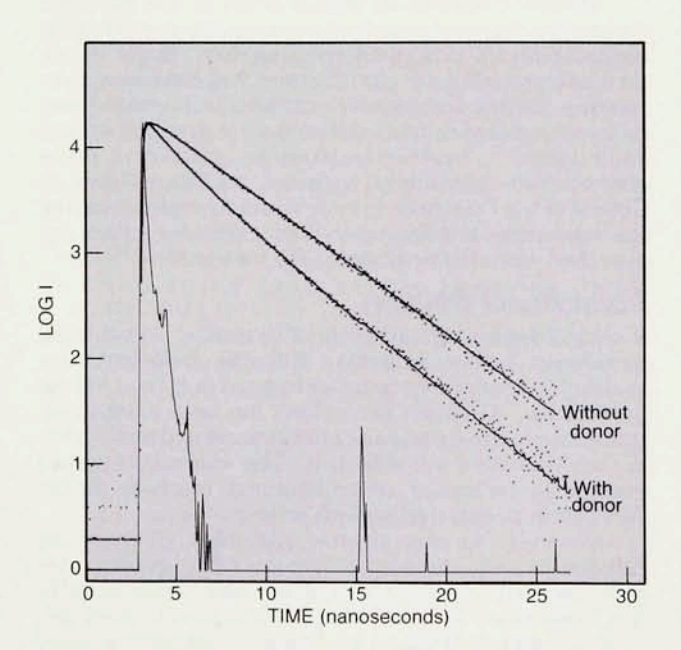
where $\langle v \rangle = (8k_{\rm B} T/\pi M)^{1/2}$ is the molecules' mean veloc-

ity, M is the molecular mass and g is a proportionality factor related to the structure of the glass, and thus depends on the porosity, tortuosity and so on. Although originally developed for a cylindrical pore, equation 6 holds in those more general cases where the pore is well characterized by $R_{\rm p}$.

In the Knudsen regime one can follow a diffusion-limited reaction in a series of porous glasses. Figure 8 shows how diffusing acceptors, or quenchers, move within the pore network and quench an initially excited adsorbed donor molecule on encountering it. In a way donor quenching due to Knudsen diffusion is analogous to donor relaxation by direct energy transfer. In energy transfer the boundaries restrict the locations of the adsorbed molecules. In Knudsen diffusion the same boundaries restrict the motion of the gas-phase acceptors. In both cases it is possible to relate the morphology to the decay pattern of the donor, which can be calculated assuming that the pore space in the glasses is a three-dimensional and homogeneous, yet tortuous, network. The donor is expected to decay exponentially with rate K given by

$$K = K_{\mathrm{q}} + \tau_{\mathrm{L}}^{-1}$$

where $\tau_{\rm L}$ is the lifetime of the isolated donor and $K_{\rm q}$ is giv-



Fluorescence decay for rhodamine 6G adsorbed onto the pore surfaces of Si-100 can be fit to a single exponential (upper curve). The lower curve shows the fluorescence decay of the adsorbed donor rhodamine 6G in the presence of the acceptor malachite green. The instrument-response spikes are also shown. Figure 7

en by a Smoluchowski expression for donor annihilation by diffusing acceptors:

$$K_{\rm q} = \left(\frac{g\langle v\rangle r_{\rm AB}}{k_{\scriptscriptstyle {
m P}}T}\right) R_{\scriptscriptstyle {
m p}} P$$

where $r_{\rm AB}$ is a reaction radius. The donor decay rate scales with $R_{\rm p}$ and with the gas pressure: Within the Knudsen regime, the larger the pore size, the more efficient is the quenching process. This mechanism breaks down for very large pores where l is much smaller than $R_{\rm p}$, the limit at which Knudsen diffusion is no longer effective, and simple diffusion of the quenchers toward the donor, dominated by l, takes over.

Experimentally, the decay of initially excited benzophenone, which is adsorbed on the pore surface and quenched by diffusing oxygen gas molecules, has been studied using time-resolved diffuse-reflectance transient absorption. 16 The quenching rates show linear dependences on both the mean pore size and the pressure,

confirming Knudsen behavior.

Molecular quenching within pores in the Knudsen regime provides an example of a monomolecular diffusionlimited reaction in a restricted geometry. Raoul Kopelman and coworkers at the University of Michigan have recently studied bimolecular reactions in restricted geometries by following delayed fluorescence in triplet-triplet annihilation.17 Another spectroscopic method to probe pore surface morphology, proposed by Pierre-Gilles de Gennes of the College de France would require measuring the relaxation of diffusing excited molecules which are quenched when they encounter the pore surface.18

Translational diffusion

A central issue of the problem of dynamics in restricted geometries is how molecular diffusion coefficients are modified in confined environments relative to their values in the bulk. Although this subject has been extensively studied for many years, basic questions related to diffusion in confined spaces are still open. The wide use of porous systems in molecular separation and catalysis makes

diffusion in porous media of major importance.

Generally we can identify a number of limits for diffusion in restricted spaces: free gas diffusion (dominated by molecule-molecule scattering) and Knudsen diffusion (dominated by molecule-pore scattering), both discussed above in relation to gas-phase quenching reactions; surface diffusion; diffusion in confined liquids; and diffusion in bulk liquids. The conditions for each of these limits vary from system to system, as do the values of the diffusion coefficients in the separate regimes of gas-filled, liquid-filled and partially filled (gas and liquid) pores. Translational diffusion in gas-filled pores has been addressed in the section on the Knudsen regime. Here we focus on liquid-filled and partially filled pores.

The study of diffusion in liquids embedded in pores has been approached by means of forced Rayleigh scattering, 19 pulsed-gradient nmr²⁰ and light scattering. 21 Because we cover here mainly optical techniques, we will describe how forced Rayleigh scattering is used for measuring molecular diffusion in solution in transparent

porous systems.

Forced Rayleigh scattering is essentially a transient grating experiment. One uses a probe molecule that undergoes photoisomerization from a trans isomer to a cis isomer with different optical properties. Two laser beams, which are crossed to create an interference pattern, are used to induce the isomerization and thereby create a refractive-index diffraction grating of periodicity L in the sample. A third laser is Bragg scattered from this grating. As the cis isomers diffuse, the grating pattern fades away, a process that is observed by the decay of the Bragg scattering. For an exponential decay in time, one can relate the time constant τ for the decay to the diffusion D of the probe molecule:

$$Dq^2 = \frac{1}{\tau} - \frac{1}{\tau_{\rm R}} \tag{7}$$

where $q = 2\pi/L$ is the wavevector of the grating and τ_R is the thermal relaxation time of the cis to trans isomerization. One can create a range of periodicities and deter-

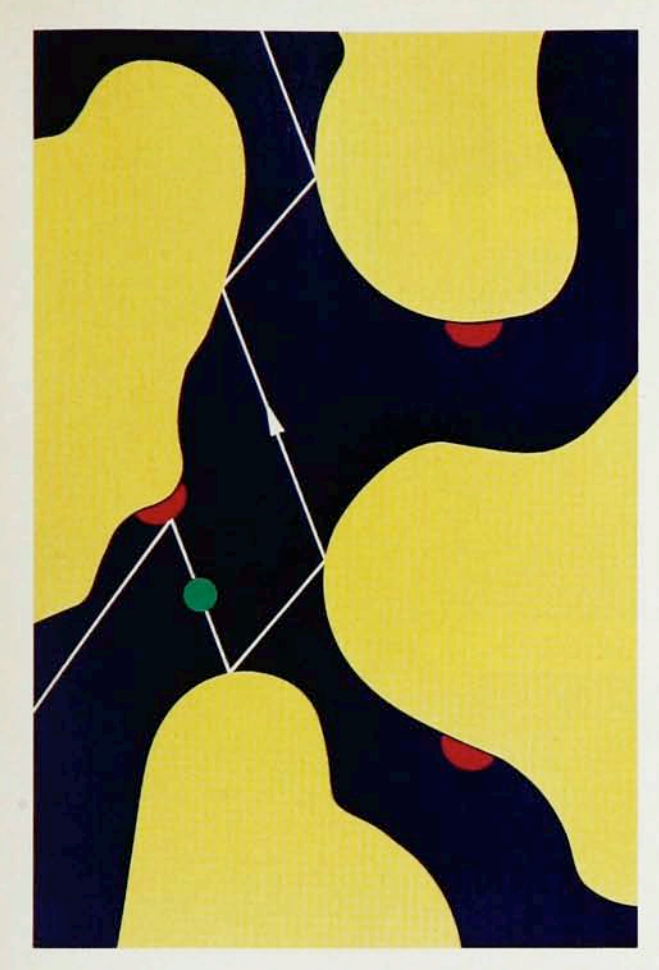
mine D from the slope of τ^{-1} versus q^2 .

In a forced-Rayleigh-scattering experiment carried out on porous vycor with azobenzene as the probe molecule,22 the diffusion coefficient obtained was approximately 10^{-8} cm 2 /sec. This means the diffusion was about 50 times slower than the diffusion of azobenzene in bulk solution. The presence of boundaries leads to the slowing down of diffusion processes in embedded liquids, as one expects from the tortuous paths within such systems and from higher effective viscosities. Again, two extreme models can be presented:

If the pore network (but not the pore surface) is fractal, then it is characterized by a fractal dimension d_s on length scales $l_1 < l < l_2$, where l_1 and l_2 are the lower and upper cutoffs of the fractal range. Because of the nature of fractal structures, the notion of tortuosity is inherent in the model. It is well established that diffusion on fractals is governed by both d_s and the spectral dimension d, a measure of the connectivity of the pore network. Beyond l₂ the pores can be described as a disordered threedimensional network. A simple calculation of forced Rayleigh scattering in the framework of this model yields, for periodicities much greater than l_2 :

$$\tau = \tau_0 \left(\frac{l_2}{l_1}\right)^{2(d_{\bullet}/\tilde{d})} \left(\frac{L}{l_2}\right)^2 \tag{8}$$

where τ_0 is the elementary step time of the molecular



Excited donor molecule (red), which is adsorbed onto the pore surface, is quenched by a gas-phase, Knudsen-diffusing acceptor molecule (green) in a porous glass. **Figure 8**

motion. From equation 7 we obtain (assuming large τ_R)

$$D = D_0 \left(\frac{l_1}{l_2}\right)^{2[(d_q/\bar{d})-1]} \tag{9}$$

where $l_1{}^2 \simeq D_0 \, \tau_0 \simeq R_{\rm p}{}^2$. D_0 is the diffusion coefficient of the molecule in the confined liquid and can be approximated by the Stokes–Einstein equation. Equations 8 and 9 offer an analysis of forced Rayleigh scattering in fractal networks. However, Vycor glass turns out not to have a fractal pore structure, and therefore equation 9 cannot account for the azobenzene diffusion.

 \triangleright The second approach assumes a cylindrical pore of radius R_p filled with liquid, within which a molecule of radius r_m diffuses. A hydrodynamic calculation leads to an equation for the molecular diffusion in terms of the ratio $\lambda = r_m/R_p$. This is known as the Renkin equation²³:

$$D = D_0(1 - \lambda^2)(1 - 2.104\lambda + 2.089\lambda^3 - 0.948\lambda^5)$$
 (10)

Here again D_0 is the molecular diffusion according to the Stokes–Einstein equation. The Renkin equation has been shown to be approximated by a simple form, $D/D_0=\exp(-4.6\lambda)$. For azobenzene in Vycor, $r_m/R_p\simeq 0.2$ and the diffusion coefficient calculated according to equation 10 is higher than the measured value, even when corrections for tortuosity are considered. Thus, the Renkin equation results in incomplete rescaling of the

diffusion of azobenzene as $R_{\rm p}$ is varied, perhaps because it does not account for the connectivity of the pore network. The fractal approach (equation 9) does try to account for pore connectivity, but fails because Vycor is neither a mass fractal nor a surface fractal. Hence the diffusion of azobenzene in Vycor remains an unsolved problem.

References

- J. W. Cahn, J. Chem. Phys. 42, 93 (1964). B. C. Bunker, D. R. Tallant, T. J. Headly, G. L. Turner, R. J. Kirkpatrick, Phys. Chem. Glasses 29, 106 (1988).
- M. W. Shafer, D. D. Awschalom, J. Warnock, G. Ruben, J. Appl. Phys. 61, 5438 (1987).
- S. J. Gregg, K. S. W. Sing, Adsorption, Surface Area and Porosity, Academic P., New York (1982). R. Sh. Mikhail, E. Robens, Microstructure and Thermal Analysis of Solid Surfaces, Wiley, New York (1983).
- 4. P. Levitz, G. Ehret, S. K. Sinha, J. M. Drake, to be published.
- H. Braumberger, P. Debye, J. Phys. Chem. 61, 1623 (1957). P. Debye, H. R. Anderson Jr, H. Brumberger, J. Appl. Phys. 28, 679 (1957). A. Guinier, G. Fournet, Small Angle Scattering of X-rays, Wiley, New York (1955).
- 6. S. K. Sinha, Physica D (Utrecht) 38, 310 (1989).
- J. M. Drake, P. Levitz, S. K. Sinha, in *Better Ceramics Through Chemistry*, C. J. Brinker, D. E. Clark, D. R. Ulrich, eds., Materials Research Society, Pittsburgh (1986), p. 305.
- P. W. Schmidt, A. Höhr, H.-B. Neumann, H. Kaiser, D. Avnir, J. R. Lin, J. Chem. Phys. 90, 5016 (1989).
- J. Warnock, D. D. Awschalom, M. W. Shafer, Phys. Rev. 57, 1753 (1986).
- J. Klafter, J. M. Drake, eds., Molecular Dynamics in Restricted Geometries, Wiley, New York (1989).
- J. Warnock, D. D. Awschalom, M. W. Shafer, Phys. Rev. B 34, 475 (1986).
- P. Debye, L. Cleland, J. Appl. Phys. 30, 843 (1985).
- 13. J. Klafter, A. Blumen, J. Chem. Phys. 80, 879 (1984).
- P. Levitz, J. M. Drake, J. Klafter, J. Chem. Phys. 89, 5224 (1988).
- E. L. Cussler, Diffusion: Mass Transfer in Fluid Systems, Cambridge U. P., New York (1984).
- J. M. Drake, P. Levitz, J. Klafter, N. J. Turro, K. S. Nitsche, K. F. Cassidy, Phys. Rev. Lett. 61, 865 (1988).
- 17. R. Kopelman, Science 241, 1620 (1988).
- 18. P.-G. de Gennes, C. R. Acad. Sci. Ser. B 295, 1061 (1982).
- F. Rondelez, H. Hervet, W. Urbach, Chem. Phys. Lett. 53, 138 (1983).
- J. Karger, J. Lenzner, H. Pfeifer, H. Schwabe, W. Heyer, F. Yankowski, F. Wolf, S. F. Zdanov, J. Am. Ceram. Soc. 65, 69 (1983). F. D'Orazio, S. Bhattacharja, W. P. Halperin, R. Gerhardt, Phys. Rev. Lett. 63, 43 (1989).
- M. T. Bishop, K. H. Langley, F. E. Karasz, Phys. Rev. Lett. 56, 197 (1986).
- W. D. Dozier, J. M. Drake, J. Klafter, Phys. Rev. Lett. 56, 197 (1986).
- 23. R. E. Baltus, J. L. Anderson, Chem. Eng. Sci. 38, 1959 (1983).